INF1 - Surface plasmons

Yannick Couzinié & Hannes Malcha

SS 2015
24.08-25.08.2015

Contents

1 Introduction

In recent years surface plasmons have received attention from the scientific community for different uses, such as wave transmitting [Kre99], [Mai02] or signal amplification [Kne97], [Nie97]. During the course of this experiment, we have examined the theory of surface plasmons and derived a few theoretical predictions, which we have then tried to confirm with several measurements.

2 Theory

In this section we are going to discuss the theory of surface plasmons and linked values. The nomenclature used from here on out is specified in Fig. 1.

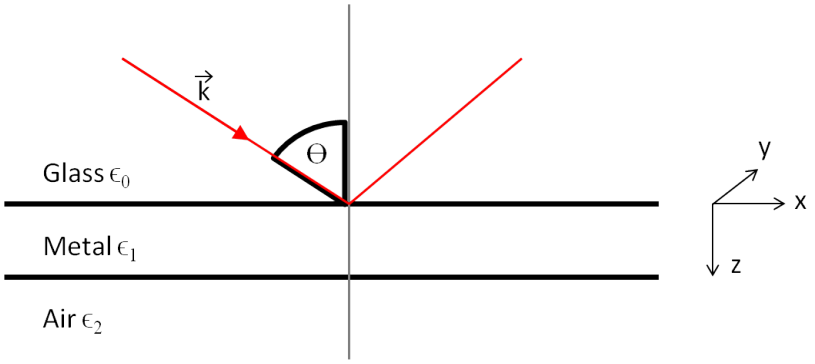

Figure 1: Draft of the Kretschmann-Raether-Konfiguration (see section 2.5.1). From now on every index 0,1,2 corresponds to the respective layer of glass, metal or air.

2.1 Permittivity

The permittivity of a material describes its reaction to and effects on electric fields.

2.1.1 Air

The permittivity of air ε_2 is in good approximation equal to 1.

2.1.2 Silver

In this experiment we will use silver samples to detect surface plasmons. The permittivity of silver is given the following empirical formula derived by Hornauer [Hor], with the wavelength λ in $\mathring{A}$:

$$\begin{aligned}\varepsilon_1(\lambda) = &- 219.954 - 0.0261695\lambda + 3.8559\sqrt{\lambda} + \frac{4857.2}{\sqrt{\lambda}} \\ &+ i(7.139 + 0.001656\lambda - 0.2129\sqrt{\lambda}).\end{aligned} \tag{1}$$

It is only accurate for wavelengths in the range from $3500\mathring{A}$ to $7000\mathring{A}$.

2.1.3 Glass

The prisms and glass samples' permittivity can be approximated by the following empirical formula derived by Nähbauer [Näh], with the wavelength λ in $\mathring{A}$:

$$\varepsilon_0(\lambda) = 2.979864 + \frac{877780.8}{\lambda^2 - 1060900} - \frac{84.06224}{96 - \lambda^2 \cdot 10^{-8}} \tag{2}$$

2.2 Surface Plasmons

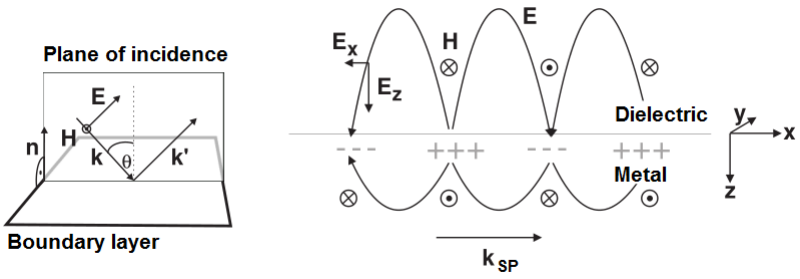

Figure 2: *Left:* p-polarized incident light is reflected at the interface of a metal and a dielectric material. *Right:* Diagram of surface plasmons at the boundary layer metal/dielectric. [Men08]

In solid metals there is a nearly free electron gas, whose density fluctuations, can lead to an excess negative charge in a region. This leads to an induced excess of positive charges in neighbouring regions, and that in turn will induce an excess of negative charges again. This wavelike charge-density fluctuation will propagate through the metal following the wave particle duality, we

identify this wave with a particle which we will refer to as plasmon. In this particular experiment we only focus on the discussion of surface plasmons, which are plasmons located at a interface between a metal and a dielectric (see Fig. 2, right side). The charge density fluctuations lead to electric fields between different regions. It is apparent from Fig. 2 that the electric field $\vec{E}$ has a component parallel to the wave vector $\vec{k}_{SP}$ of the surface plasmons (E_x) and one perpendicular to it (E_z).

2.3 Dispersion relation

In order to excite surface plasmons the wave vector as well as the wavelength of the incident light and the surface plasmons need to match. Therefore we will need to know the dispersion relations of light and surface plasmons.

2.3.1 Dispersion relation of light

The dispersion relation of light in a medium with permittivity ε is given by

$$k = \frac{\omega}{c_0}\sqrt{\varepsilon}. \tag{3}$$

But since we are only interested in the x-component (see Fig. 1) of the wave vector, we use the projection on the x-axis and obtain

$$k_x = \frac{\omega}{c_0}\sqrt{\varepsilon}\sin(\theta). \tag{4}$$

2.3.2 Dispersion relation of surface plasmons

As we can see in Fig. 2 the electromagnetic wave that is bound to the surface plasmon has the following form

$$\vec{E}_i = \begin{pmatrix} E_{xi} \\ 0 \\ E_{zi} \end{pmatrix} \cdot e^{i(k_{zi}\cdot z + k_{xi}\cdot x - \omega t)} \quad \vec{H}_i = \begin{pmatrix} 0 \\ H_{yi} \\ 0 \end{pmatrix} e^{i(k_{zi}\cdot z + k_{xi}\cdot x - \omega t)}. \tag{5}$$

The wave vector consists of 2 components and with equation 3 we retrieve

$$\varepsilon_i \frac{\omega^2}{c_0^2} = k^2 = k_{xi}^2 + k_{zi}^2. \tag{6}$$

With Maxwell's equations we then accede to

$$k_x = \frac{\omega}{c_0}\sqrt{\frac{\varepsilon_1 \cdot \varepsilon_2}{\varepsilon_1 + \varepsilon_2}}. \tag{7}$$

2.4 Evanescent wave

Whenever light incides on a boundary layer between two materials at an angle θ,reflection occurs. Following from equations 4 and 6, for angles of incidence higher than

$$\theta_{tot} = \arcsin\left(\sqrt{\frac{\varepsilon_2}{\varepsilon_1}}\right) \tag{8}$$

incident light is totally reflected and the z-component of the k_2-vector becomes imaginary, thus the light wave is exponentially dampened. This is referred to as an evanescent wave. The angle θ_{tot} is referred to as the total reflection angle.

2.5 Exciting surface plasmons

Surface plasmons can be excited in two different ways. It is assumed from now on that the incident light is polarised as shown in Fig. 2. This polarisation is referred to as p-polarisation, meaning that the electric field vector is parallel to the plane of incidence.

2.5.1 Kretschmann-Raether-method

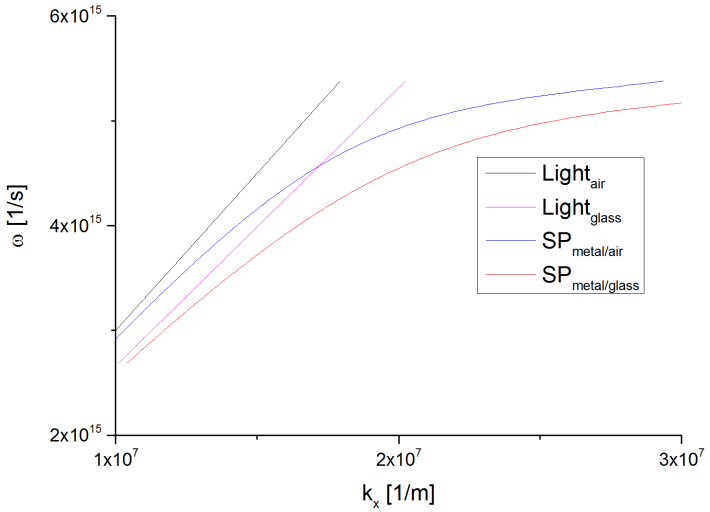

Figure 3: Dispersion relations $\omega(k_x)$ of light and surface plasmons, according to the equations 4 and 7 plotted in the same graph.

As observable in Fig. 3 it is not possible to excite surface plasmons on the metal/air interface with light that propagates through air, since the dispersion relations of light and surface plasmons do not have a point of intersection. Apparent from equation 4 any dispersion relation of light propagating in a material with a higher permittivity than air will have a point of intersection with the dispersion relation of the metal/air surface plasmons.

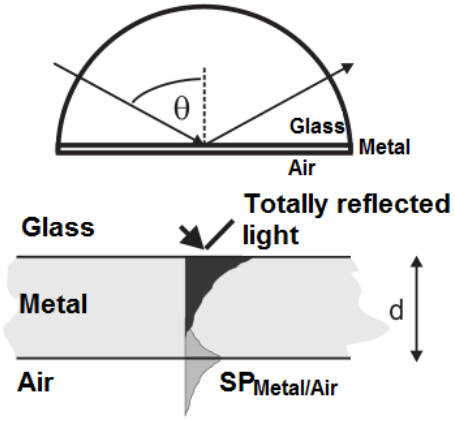

Figure 4: Kretschmann-Raether-configuration [Men08]

Fig. 4 shows a possible configuration using light that propagates through glass to excite metal/air surface plasmons. This is achieved by having a metal layer (we used 20-70nm thick silver probes) on the flat side of a glass prism and air on the other side, as depicted in Fig. 4. By shining the incident light wave under an angle θ, that is higher than the total reflection angle θ_{tot}, only an exponentially damped evanescent wave is transmitted through the metal. The k_x-vector of this evanescent wave is conserved throughout the transmission, and if the metal layer is thin enough, the evanescent wave reaches to the metal/air layer boundary and can excite a surface plasmon there, with the frequency ω and wave vector k_x according to the point of intersection seen in Fig. 3.
It is possible to derive a formula from the Fresnel-equations for the total reflectivity r_{012} for the glass-metal-air system from the fresnel equations, which respects multiple orders of reflection leading to a geometric series. We

obtain

$$r_{012} = \frac{r_{01} + r_{12} \exp\left(2ik_{z1}d\right)}{1 + r_{01} \cdot r_{12} \cdot \exp\left(2ik_{z1}d\right).} \tag{9}$$

Whereby we chose the notation r_{012} to indicate that it is the reflectivity index from light reflected at the glass/metal(01)- and the metal/air(12)-interfaces.

2.5.2 Lattice-Method

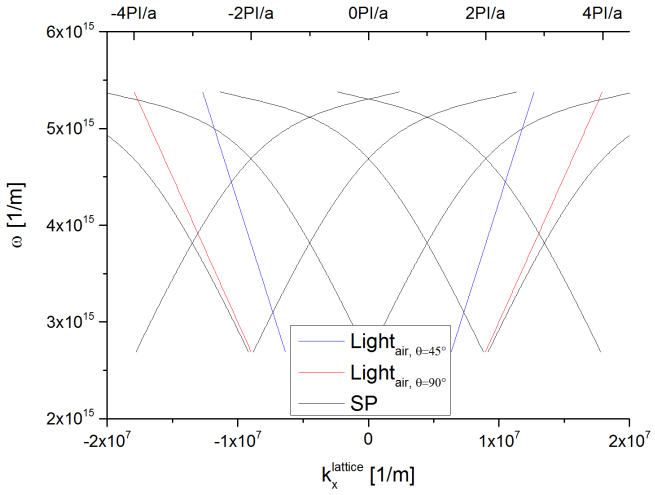

Figure 5: Dispersion relation of surface plasmons on a modulated silver film.

Using an undulated metal sample instead of a flat one, it is possible to excite plasmons with light propagating through air.
As opposed to the flat situation, where we saw in Fig. 3 that the dispersion relations do not have a point of intersection, we now see a dispersion relation of the surface plasmons akin to the electronic band structure of solids. Due to the periodicity of the silver film we obtain the dispersion relation observable in Fig. 5 and we see that we now get multiple points of intersection between the dispersion relations for any angle of incidence θ, which can be seen in Fig. 5. As usual we can expect band gaps at the borders of the brillouin zones.
Thus it is possible to excite plasmons in undulated samples simply by shining light on them.

3 Experiment

In this section we are are going to discuss the experimental setup.

3.1 Experimental setup

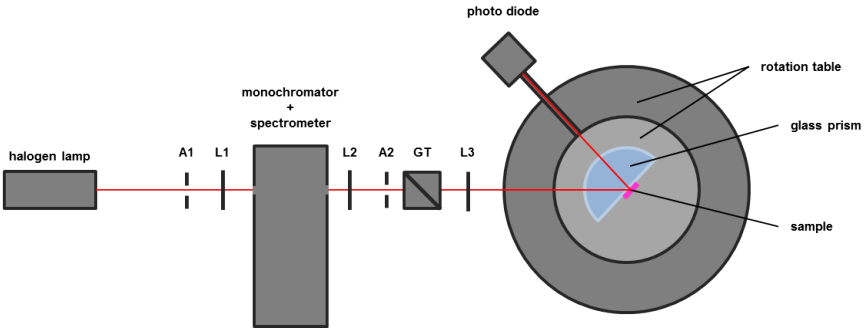

Figure 6: Draft of the experimental setup. A stands for aperture, L for lens and GT for Glan-Thompson prism

The experimental setup we used for the first part of the experiment, can be seen in Fig. 6. First we focussed the collimated light of the Halogen lamp onto the input slit of the monochromator. We used an exterior spectrometer to determine what wavelengths are transmitted through the monochromator. The monochromator is a prism-based spectrometer with a slit to let only a part of the spectrum through. This nearly monochromatic light is then collimated through the lens L2 and polarized by a Glan-Thompson prism (GT).
The Lens L3 is a concave lens which is implemented in order to mitigate the curvature effects of the following prism. This glass prism is mounted on a rotating table in the $\theta - 2\theta$ configuration. Meaning that while the prism rotates about an angle θ the photodiode rotates two times that angle, ensuring that the reflection of the prism constantly hits the detector.
A half-cylindrical prism was used in order to have a perpendicular angle of incidence for the light entering the glass, only at the prism/sample interface we get noteworthy reflection phenomena.
The samples are silver layers which were vacuum-metallized onto a glass layer. This glass layer is brought onto the prism through the help of immersion oil, which has the same index of refraction as the prism, so that the evanescent wave does not cross another air/glass boundary layer.

For the second part of the experiment, the prism/sample combination was exchanged for a undulated silver sample. Everything apart from the halogen lamp, aperture A1 and the Lens L1 was enclosed in a box, to prevent room light from interfering with the measurement.
Finally we used a photo diode to measure the intensity of the reflected light, by measuring a voltage.

3.2 Data acquisition

First the wavelength is set with the help of the monochromator. Then the rotation table was set to an appropriate angle for the corresponding measurement and using a measurement program, by letting the rotation table turn , we gather the measurement data, which consists of the voltage measured by the photo diode and the angle measured by the rotation table. At an appropriate angle we stop the measurement and repeat the process, with a different setting.

4 Results & Discussion

In this section we are going to discuss and evaluate the measurement data gathered through various measurements.

4.1 Gauging

Before we can use the experimental setup properly we need to calibrate the rotation table since the angle display is not gauged. Therefore we measure the angle of total reflection of the prism for five different wavelengths from $500nm$ to $600nm$. We then plot the graph for each measurement and determine the angle of total reflection by simply fitting two linear curves to the measurement. We obtain the total-reflection angles corresponding to their respective wavelengths which we juxtapose to the theoretical value. This can be examined in Table 1.

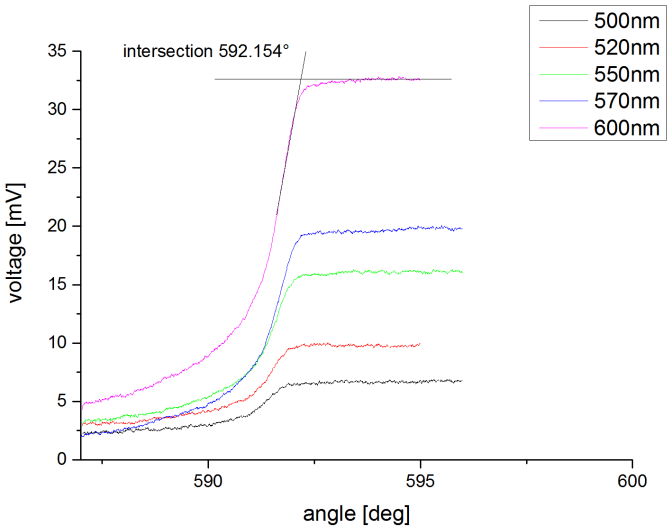

Figure 7: Measurement of the angle of total reflection for five different wavelengths from 500nm to 600nm using the setup shown in Fig. 6 but without any sample.

Experimental values [deg]	Theoretical values [deg]
591.81	43.142
591.84	43.188
592.01	43.231
592.06	43.261
592.15	43.301

Table 1: Juxtapose of experimental and theoretical values for the angle of total reflection to calculate the angle offset. Theoretical values from equation 8.

The experimental value in Tab. 1 is the 2θ value, hence we have to subtract two times the theoretical value to get the angle offset and we then obtain

$$\theta_{off} = 505.53^\circ \pm 0.03^\circ$$

. We will use this offset to correct the measured angles in all further graphs and calculations.

4.2 Kretschmann-Raether-method

In this section we will do the first experiment to prove the existence of surface plasmons using the Kretschman-Raether-method to excite them.

4.2.1 Dispersion relation

At first we measure the reflectance for six different silver samples, with a thickness ranging from $20nm$ to $70nm$, dependent on the angle range. Therefore we set up the experiment as seen in Fig. 6. Based on the theoretical discussion we would assume to see each curve drop at a certain angle θ at which plasmons are excited. Since the excitation uses energy from the incoming light, the measured reflection on the photodiode will decrease. For greater angles the curve rises again as the dispersion relation curves no longer intersect. We should see that the minima for thicker samples are not as deep because the evanescent wave does not pass through to the metal/air interface. We also do not expect deep drops in the measured reflectivity for thin samples because the surface plasmons immediately decay into light again, which then get measured by the photodiode. These expectations can vaguely be confirmed by our measurement.

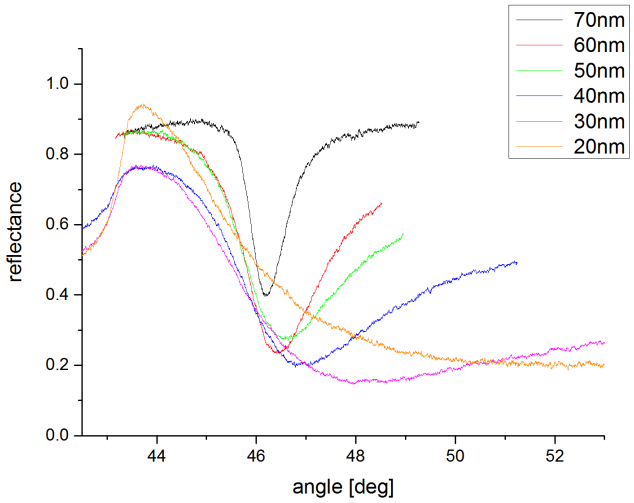

Figure 8: Measurement of the reflectance dependent on the angle of incidence of light at $550nm$ on the sample for six different samples.

To evaluate the data we use a Mathematica script to fit each curve to equation 9 with the free parameters d, Reε_1 and Imε_1. An example can be seen in Fig. 9.

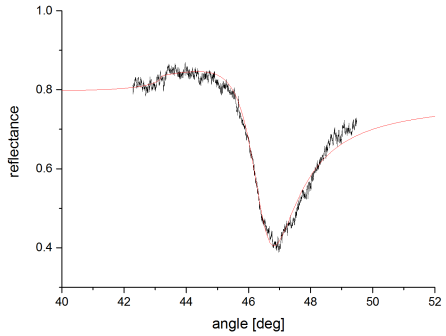

Figure 9: Fit curve for the $60nm$ sample with light at a wavelength of $520nm$.

To verify that our fit is good we compare the theoretical values for thickness and permittivity with those we received from Mathematica. For Fig. 9 this is shown in Tab. 2.

	Theoretical	Experimental
d [nm]	60.00	60.75
Re$(\varepsilon_1)[\frac{As}{Vm}]$	-10.612	-6.65
Im$(\varepsilon_1)[\frac{As}{Vm}]$	0.40	1.68

Table 2: Comparison of the theoretical and calculated values for the thickness and permittivity obtained from the Mathematica fit for the $60nm$ sample at a wavelength of $520nm$ (Fig. 9.

In Tab. 3 we have compared all values for the thickness to their corresponding theoretical values, using the measurement data shown in Fig. 8.

Theoretical [nm]	Fit curve [nm]
20	19.15
30	32.20
40	38.90
50	51.56
60	53.18
70	60.01

Table 3: Comparison of the theoretical value and the calculated value for the thickness obtained from the Mathematica fit for each sample, using the measurement data shown in Fig. 8. Fig 8 was evaluated using Mathematica 10.

As the $60nm$ sample showed the reflectivity curve that most corresponded to our expectations. We continued the measurements with this sample and repeat the whole process and change the wavelength instead.

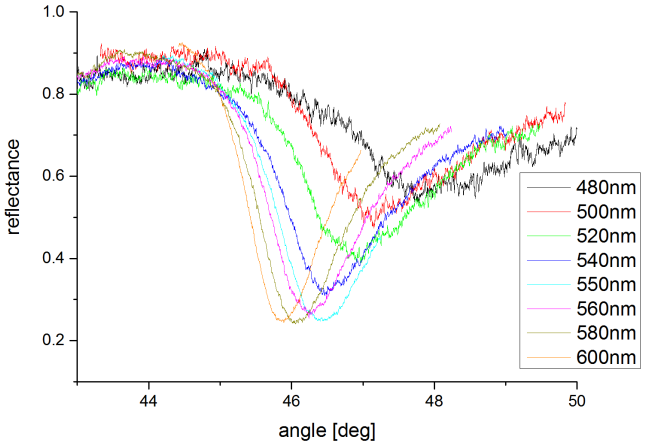

Figure 10: Measurement of the reflectance dependent on the angle of incidence of light on the sample for eight different wavelengths and the $60nm$ sample. Including the $60nm$ measurement from Fig. 8.

We immediately see that the drops appear at greater angles for lower wavelengths, which is in accordance with the expectations from Fig. 3. Beside the Mathematica fitting we also measure the minimum for each curve by fitting it around the minimum. We obtain the following angles for the minima.

Wavelength [nm]	Angle [deg]
480	47.85
500	47.19
520	46.81
540	46.43
550	46.36
560	46.22
580	45.98
600	45.84

Table 4: Minima of the reflectance curves for eight different wavelengths. Fig 10 was evaluated using Origin Pro 9.1

We then calculate the frequency ω from the wavelength and use equation 4 to calculate k_x from the angles and plot the points together with the theoretical graph from Fig. 3 for the dispersion relation for surface plasmons on the metal air boundary layer. As expected we see that the dispersion relation of light in air does not cross the dispersion relation of the surface plasmons at the metal/air interface.

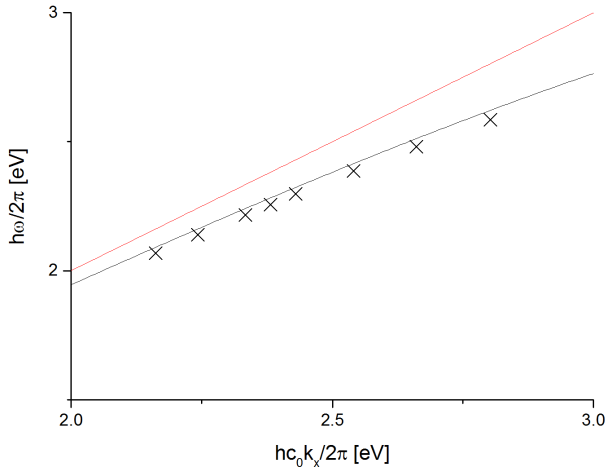

Figure 11: Theoretical (line) and measured (crosses) dispersion relation for surface plasmons at the boundary metal air. In red we see the dispersion relation of light in air.

All our measured points are below the theoretical graph. Therefore we assume that we have systematic errors (e.g. measured the wrong offset angle) or an erroneous sample (e.g. a silver-oxide layer on the surface) in our experimental setup. On average the measured values are $(33 \pm 8)meV$ below the corresponding theoretical value.

4.2.2 Permittivity

We will now evaluate the data for Reε_1 and Imε_1, using the values from Fig. 10. Subsequently we plot the permittivity from equation 1 separated for the real and imaginary part of ε_1 together with our results from the fitting.

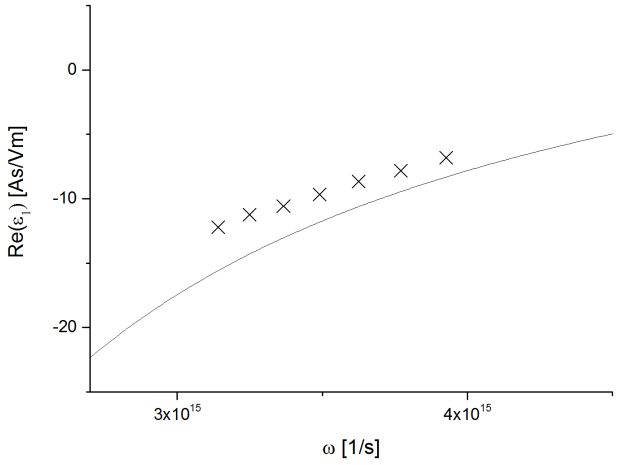

Figure 12: Theoretical plot (line) of the real part of equation 1 and the related values from the Mathematica script (crosses) with the data from Fig. 10.

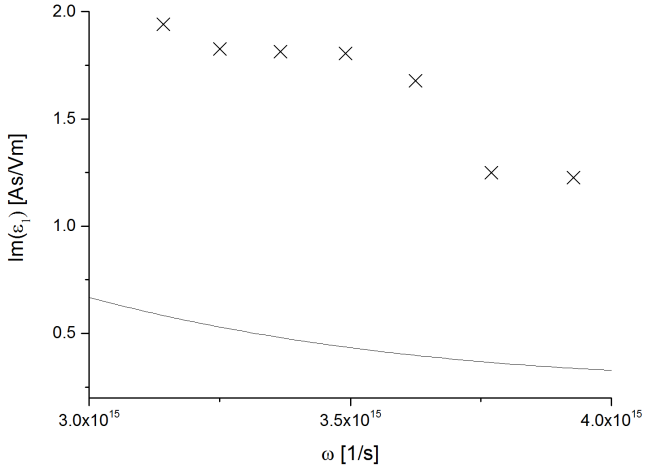

Figure 13: Theoretical plot (line) of the imaginary part of equation 1 and the related values from the Mathematica script (crosses) with the data from Fig. 10.

For the real part the experimental values are at average $(2.3 \pm 0.7)\frac{As}{Vm}$ higher than the theoretical curve and for the imaginary part they are $(1.2 \pm 0.2)\frac{As}{Vm}$ higher. Again it is safe to say we have to deal with a systematic error or an erroneous sample as discussed before, hence all measured points are above the theoretical curve.

4.3 Lattice-method

In this sub-section we use an undulated silver sample to measure the dispersion relation of the metal/air surface plasmons in lattices. For this we use the experimental setup depicted in Fig. 6 with a undulated silver sample instead of the prism.

4.3.1 Lattice-constant

Since we do not know the lattice-constant of the lattice used in the experiment, we have to determine that first.
Lattices diffract light, so by measuring the angle differences between the main and the first orders of diffraction you can calculate the lattice-constant

a with the following formula

$$a = \frac{\lambda}{\sin(|\Delta\theta|)}. \tag{10}$$

The angle measurements are achieved by reflecting the main order of diffraction back into the monochromator,taking this as the main order angle (read from the angle display on the rotation table) and marking the angles for the first orders of diffraction. Following this we rotate the table letting the main order of diffraction fall onto the location where the first order of diffraction was before, so that the angle display on the table now shows the angle corresponding to the first order of diffraction. By subtracting both angles we get the needed angle difference and the results can be seen in Tab. 5.

	Angle [deg]
Main OOD	590
1st OOD left	654.93
1st OOD right	525.5

Table 5: Measured angles for the 0th and the first order of diffraction (OOD).

We then obtain a value for the lattice constant of

$$a = (699 \pm 1)nm$$

4.3.2 Dispersion relation in a lattice

Analogously to section 4.2 we are now going to measure the dispersion relation. As opposed to that measurement, we expect two minima in this measurement. This can be explained with Fig. 5. The wave vectors we examine in our measurements are close to one of the intersections of the different orders of the dispersion relation thus by cycling through the angles we expect two points of intersection of the dispersion relations and as such, two points where light gets absorbed as surface plasmons and we expect minima.

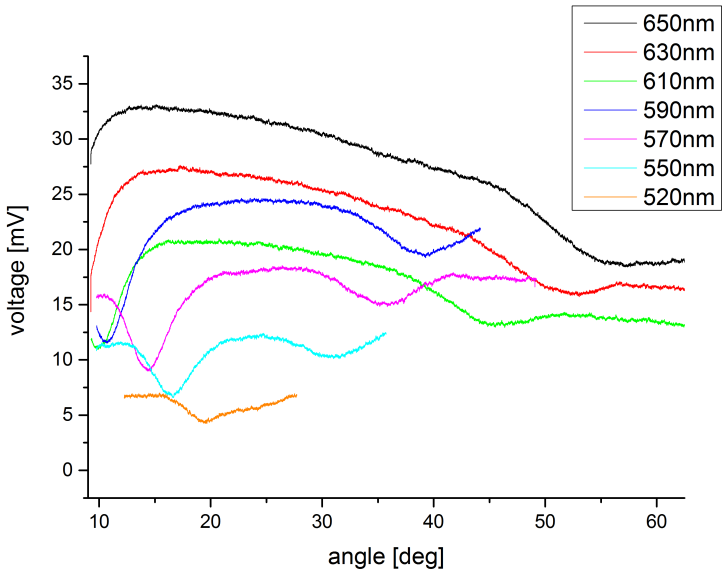

Figure 14: Measurement of the reflection dependent on the angle of incidence of light on the sample for seven different wavelenghts specified in the figure, for the undulated silver sample.

In Fig. 14 we see the expected results. The black curve, being the curve for the measurement with a wavelength of $650nm$, can not be examined as the minima are not detectable in the angle range we measured. The decrease at approximately 90° is one of the expected points, but the following angle is so high, that the incident light does not correctly hit the lattice anymore, thus leading to a constant minimal measured value.

Wavelength [nm]	1st PMT [deg]	2nd PMT [det]
630		52.88
610	9.722	46.045
590	10.584	39.166
570	15.104	35.388
550	16.347	30.891
520	19.522	

Table 6: Measured angles for the two points of minimal turning (PMT) for 7 different wavelengths specified in the table. The PMT were evaluated using the software Origin Pro 9.1.

The $630nm$ curve clearly shows two points of minimal turning even though the first one is not measured as it is located at angles too small for our setup. The $610nm, 590nm, 570nm, 550nm$ all show the expected two points of minimal turning for angles displayed in Table 6, and we can clearly see that for decreasing wavelengths, and as such increasing wave vectors k_x and frequencies ω, the angle difference between the two points of minimal turning decreases. And the $520nm$ curve only shows one point of minimal turning, at this point we have come to the crossing between two curves.
Using the equations $\omega = \frac{2\pi c_0}{\lambda}$ and 4 with $\varepsilon_2 = 1$ we can compare these measurements to the theoretical expectation seen in Fig. 5. The results can be observed in Fig. 15.

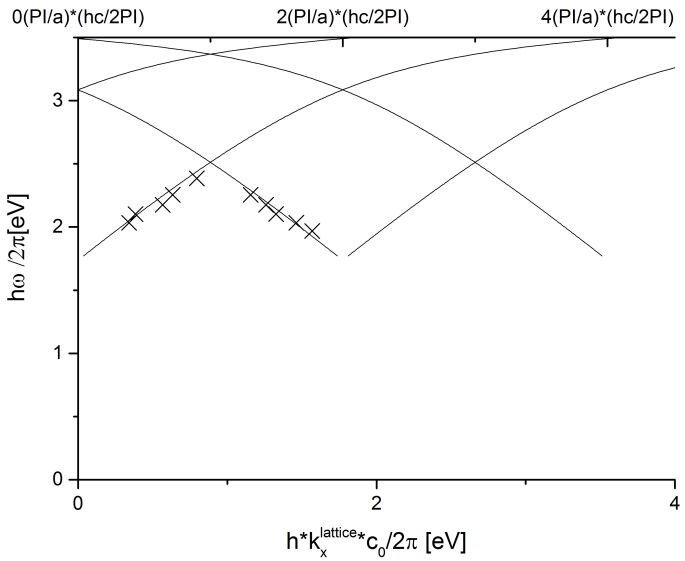

Figure 15: Measurement of the reflection dependent on the angle of incidence of light on the sample for seven different wavelengths specified in the figure, for the undulated silver sample. The theoretical plot is only made for wavelengths in the range specified for equation 1.

We see a strong correlation between the measured points and the theory. The previously discussed reasons for offset are not observable anymore. This suggests that we do not have a systematic error in our setup, but rather that the previous samples had the discussed silver-oxide layer altering the permittivity curve. Considering these results it is likely that we have excited surface plasmons.

5 Conclusion

With the results of the evaluations and taking into consideration the erroneous samples discussed in their respective chapters, we saw that both methods have yielded good results.
As discussed the first measurements showed offsets presumably due to a silver-oxide layer on the samples. Despite that the tendency of the theoretical curves were clearly visible.
From the lattice-method we obtained results with minimal offset from the theoretical curves.
As a final conclusion we can say with great certainty that we have observed and excited surface plasmons on silver samples.

References

[Hor] D.L. Hornauer.

[Kne97] K. Kneipp, Y. Wang, H. Kneipp, L.T. Perelman, I. Itzkan, R.R. Dasari and M.S. Feld. *Single Molecule Detection Using Surface-Enhanced Raman Scattering (SERS).* Phys. Rev. Lett. 78, 1667 (1997).

[Kre99] J.R. Krenn, A. Dereux, J.C. Weeber, E. Bourillot, Y. Lacroute, J.P. Goudonnet, G. Schider, W. Gotschy, A. Leitner, F.R. Aussenegg and C. Girard. *Squeezing the Optical Near-Field Zone by Plasmon Coupling of Metallic Nanoparticles.* Phys. Rev. Lett. 82, 2590, 1999.

[Mai02] S.A. Maier, P.G. Kik and H.A. Atwater. *Observation of coupled plasmonpolariton modes in Au nanoparticle chain waveguides of different lengths: Estimation of waveguide loss.* Appl. Phys. Lett. 81, 1714 (2002).

[Men08] S. Mendach and M. Böll, *Oberflächenplasmonen Script*, Fortgeschrittenenpraktikum, Institut für Angewande Physik, Universität Hamburg, Ver. 3, 2008.

[Näh] Nähbauer.

[Nie97] S.M. Nie and S.R. Emery. *Probing single molecules and single nanoparticles by surface enhanced Raman scattering.* Science 275, 1102 (1997).